LAWRENCE
LIVERMORE
NATIONAL
LABORATORY

UCRL-JRNL-225803

Fabrication of Double Shell Targets with a Glass Inner Capsule Supported by SiO2 Aerogel for Shots on the Omega Laser in 2006

M. Bono, D. Bennett, C. Castro, J. Satcher, J. Poco, W. Brown, H. Martz, N. Teslich, R. Hibbard, A. Hamza, P. Amendt, H. Robey, J. Milovich, R. Wallace

November 3, 2006

Fusion Science and Technology

Fabrication of Double Shell Targets with a Glass Inner Capsule Supported by SiO_2 Aerogel for Shots on the Omega Laser in 2006

August 4, 2006

Matthew Bono, Don Bennett, Carlos Castro, Joe Satcher, John Poco, Bill Brown,
Harry Martz, Nick Teslich, Robin Hibbard, Alex Hamza, Peter Amendt,
Harry Robey, Jose Milovich, Russell Wallace

ABSTRACT

Indirectly driven double shell implosions are being investigated as a possible noncryogenic path to ignition on the National Ignition Facility. Lawrence Livermore National Laboratory has made several technological advances that have produced double shell targets that represent a significant improvement to previously fielded targets. The inner capsule is supported inside the ablator shell by SiO_2 aerogel with a nominal density of 50 mg/cm^3. The aerogel is cast around the inner capsule and then machined concentric to it. The seamless sphere of aerogel containing the embedded capsule is then assembled between the two halves of the ablator shell. The concentricity between the two shells has been improved to less than 1.5 μm. The ablator shell consists of two hemispherical shells that mate at a step joint that incorporates a gap with a nominal thickness of 0.1 μm. Using a new flexure-based tool holder that precisely positions the diamond cutting tool on the diamond turning machine, step discontinuities on the inner surface of the ablator of less than 0.5 μm have been achieved. New methods have been used to comprehensively characterize each of the targets using high-resolution x-ray imaging systems.

I. INTRODUCTION

This paper describes the development of a process for fabricating double shell targets for shots on the Omega laser in August 2006. Double shell targets are being studied as a possible noncryogenic path to ignition. The double shell ignition design for the National Ignition Facility (NIF) consists of a low-Z outer shell that absorbs hohlraum-generated x-rays, implodes, and then collides with a high-Z inner shell containing the fuel [1]. As a prelude to fielding ignition double shell targets on NIF, efforts are underway to field scaled ignition-like double shells on the Omega laser facility. Double shell targets shot on the Omega laser in 2003 produced encouraging results but identified several design aspects that could be changed to potentially improve performance [1], [2]. Many of these changes were incorporated into the current targets. As is often the case with laser targets, the design of the double shell targets was constrained by the ability to fabricate and assemble the components with the required precision [3]-[6]. This paper describes the design of these double shell targets and the development of the manufacturing process for the targets. The design of the double shell targets that was developed in this study appears in Figure 1.

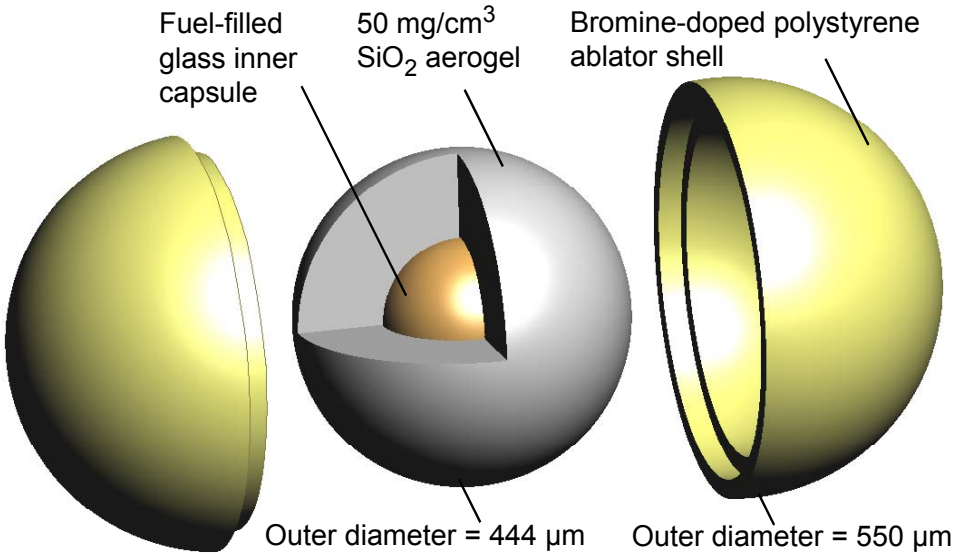

Figure 1. Exploded view of the double shell target

Several manufacturing capabilities had to be developed, and many issues had to be resolved before arriving at the final design for the targets. This design differs from previous targets in several important ways. The plastic inner shell used in the previous targets has been replaced with a glass capsule with an outer diameter of 222 μm and a thickness of 8 μm, which is filled with 62 atm of deuterium. The capsule is supported inside the ablator shell by SiO_2 aerogel with a nominal density of 50 mg/cm^3. This aerogel material has different machining characteristics than the carbonized resorcinol formaldehyde (CRF) aerogel that was used in the previous targets. Studies were performed to determine if it could be machined with a diamond tool, and if it is sufficiently robust to survive the assembly process.

The ablator shell has an outer diameter of 550 μm and a thickness of 53 μm and is composed of 2 atomic% bromine-doped polystyrene. As with the previous targets, the outer shell consists of two hemispherical components that mate at a step joint. The two ablator components are designed to mate flush with each other on the inner portion of the step joint. On the outer portion of the step joint, there is a gap between the components that is partially filled with adhesive. The design of the target is extremely sensitive to spherical asymmetries, particularly radially oriented features, and one of the factors that was hypothesized to have limited the performance of previous targets was the asymmetry created by the 2 μm gap in the joint between the two ablator components. Another study was performed to analyze the design of the joint and minimize the asymmetry that it creates. The result was a gap with a nominal thickness of 0.1 μm, or 5% of the previous value.

The ability to fabricate precise targets was limited by the lack of a capability to adequately metrologize components before they were assembled. As the manufacturing process was being developed, high-resolution x-ray digital radiography and computed tomography systems were used to characterize assemblies. These x-ray systems provided the feedback necessary to identify and fix several potential problems with the target assemblies at various stages of the manufacturing process. The result was a set of targets that met all of the specifications set by the physicists and represented a significant improvement to previously fielded double shell targets.

II. FABRICATION REQUIREMENTS

The current targets used some materials that had never been used previously in double shells. These materials made the targets sensitive to asymmetries, so the tolerances for these targets were stricter than those for previous double shells. The ablator shell had to have a wall thickness of 53±1 μm, and any radial features on the interior of the ablator had to be smaller than 0.5 μm. Therefore, the two halves of the ablator shell had to mate precisely and could not be offset from each other in the radial direction by more than 0.5 μm. The two halves of the ablator shell had to mate at a step joint that included a gap with a nominal thickness of 0.1 μm, which was partially filled with adhesive. The peak-to-valley surface finish (R_t) of the ablator shell had to be less than 100 nm. The aerogel that supported the inner capsule could not contain any voids with a dimension in the radial direction larger than 10 μm, and the surface roughness of the aerogel had to be 5 μm or better. The aerogel had to support the inner capsule concentric to the inner surface of the ablator to better than 3 μm. Meeting these specifications required the development of a novel manufacturing process.

III. OVERVIEW OF THE MANUFACTURING PROCESS

The design of these targets was intended to improve the physics performance, but it was governed primarily by the ability to fabricate them with the required precision. Several previous researchers have fabricated double shell targets with varying degrees of success, and a variety of different manufacturing processes have been reported in the literature [3]-[6]. The current effort used a manufacturing strategy very similar to the approach developed at Lawrence Livermore National Laboratory in recent years [2]. Schematic illustrations of the basic outline of the manufacturing plan appear in Figure 2 and Figure 3. These two figures will be referred to several times throughout the remainder of this manuscript.

The manufacturing process began with a glass inner capsule, which is described in Section IV of this paper. This glass inner capsule was cast inside a solid block of SiO_2 aerogel of density of 50 mg/cm^3. Section V of this paper describes how the aerogel was then diamond turned to a sphere of diameter 444 μm concentric to this embedded capsule. Section VI describes the machining of the ablator components from rods of 2 atomic% bromine-doped polystyrene. Using a diamond turning machine, the internal hemispherical surface of each ablator component was machined along with the step joint where the two halves met. Section VI also describes the development of the step joint and the tests that were performed to select a method for bonding the ablator components together. As shown in Figure 2, each target was assembled before the exterior surface of the ablator was machined. To assemble the target, one of the ablator components was placed into a special assembly station (Figure 2a), and then the sphere of aerogel containing the inner capsule was placed inside the hemispherical cavity in the ablator component (Figure 2b). Next, the other ablator component was placed on top (Figure 2c), and adhesive was applied to the interface between the ablator components. The adhesive wicked into a gap in the step joint to bond them together.

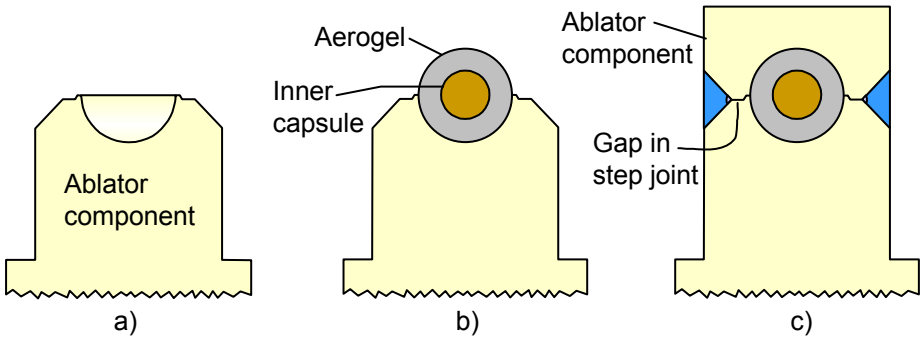

Figure 2. Schematic illustration of the assembly of a target

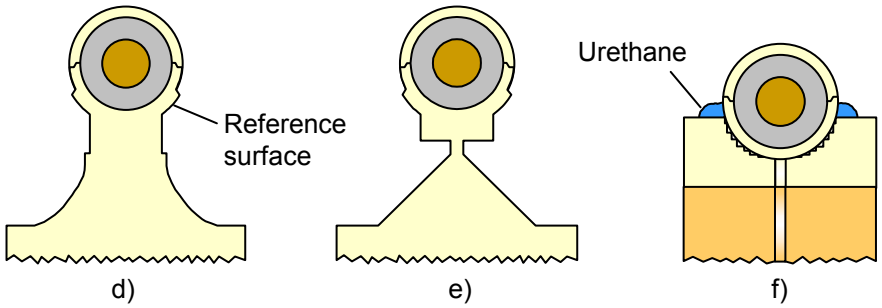

Figure 3. Schematic illustration of the machining of the exterior of the ablator

The bonded assembly was then placed back on the diamond turning machine, where the exterior surface of the ablator was machined. As shown in Figure 3d, the free end of the assembly was first machined in the form of a partial spherical shell with a wall thickness of 53 μm. This spherical shell was supported by a neck of material. In the next step, this neck was reduced to a diameter of approximately 100 μm (Figure 3e), which was then broken off to release the target. The target was then placed in a spherical vacuum chuck, where it was held in place by a small bead of urethane adhesive. The remainder of the exterior of the ablator was then diamond turned to complete the target (Figure 3f).

The remainder of this report provides a detailed description of each of the steps in the manufacturing process.

IV. INNER CAPSULE

The inner capsules used in the targets were manufactured by General Atomics. Each capsule was composed of SiO_2 glass and nominally had an outer diameter of 222 μm and a wall thickness of 8 μm. The diameter and wall thickness of each capsule used in the targets were measured with an interferometer, and the outer diameters ranged from 210 to 233 μm. The wall thickness ranged from 7.9 to 9.1 μm, and each capsule had a wall thickness uniformity of 0.2 μm or better. The surface finish of the inner capsule was critical to the experiment, so the capsules had to be as smooth as possible. The surface finish of each capsule was measured by General Atomics using an atomic force microscope-based profilometer [7], and the smoothest available capsules were used in the targets. Due to variations in the composition of the glass, some of the capsules were transparent and colorless, and some had a slightly brown color.

V. AEROGEL SUPPORT STRUCTURE

The glass inner capsule was supported inside the ablator by a structure composed of SiO_2 aerogel of density 50 mg/cm^3. The method used to fabricate this aerogel structure differed from methods that had been used in the past.

V.a. Previous Methods

In previous double shell targets, freestanding hemispheres of aerogel or foam were fabricated with an inner diameter equal to the outer diameter of the inner capsule, and the outer diameter matched the inner diameter of the ablator shell. An exploded view of such a target design appears in Figure 4. To assemble the components, the lower ablator component was first placed into a special assembly station, and then one of the aerogel hemispheres was placed into its interior. The inner capsule was then placed into the cavity in the aerogel hemisphere. The other aerogel hemisphere was then placed on top of the capsule. Finally, the upper ablator component was placed on top to complete the assembly [2].

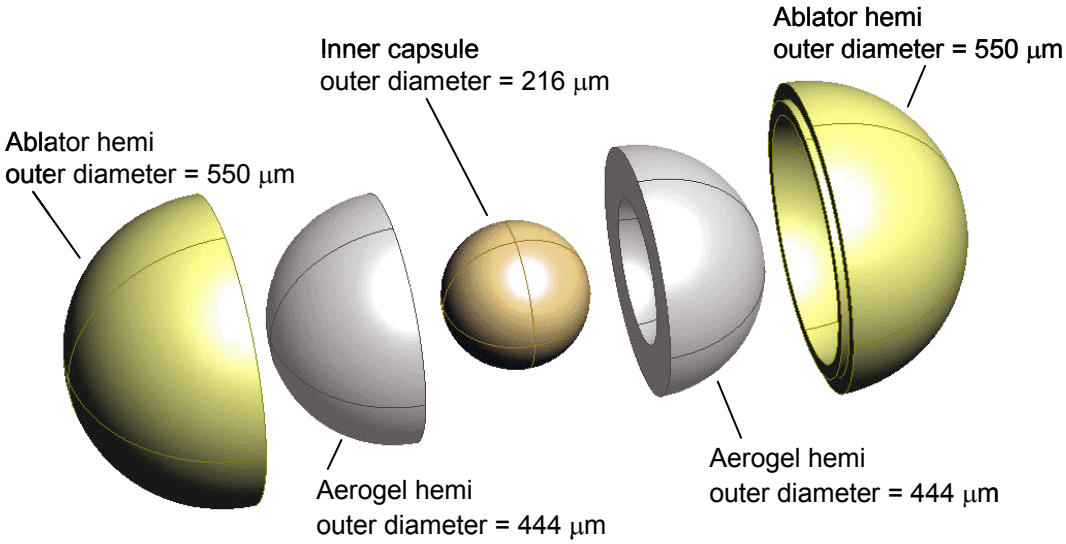

Figure 4. Exploded view of a previous design for the double shell targets

Double shell targets manufactured using this assembly method performed relatively well in laser shot experiments [1], [2]. Therefore, the plan at the onset of the current effort was to fabricate double shell targets using this same machining and assembly process. However, the new design called for 50 mg/cm^3 SiO_2 aerogel in place of the carbonized resorcinol formaldehyde (CRF) that had been used in the past.

Diamond turning hemispheres from a 6 mm diameter rod of fragile 50 mg/cm^3 SiO_2 aerogel required special procedures to machine and handle it adequately. One challenge was created by the fact that it is nearly transparent and had to be well illuminated. Reflecting a lamp off of a piece of paper placed behind the aerogel produced adequate illumination. The material was machined on a Precitech Nanoform 200 diamond turning machine equipped with a B-axis, using a single point diamond tool with a nose radius of 5 μm. Several tests were performed to identify acceptable cutting parameters for the material. All machining was performed with a spindle speed of 1700 rpm and a depth of cut of 1 to 3 μm for roughing cuts and 1 μm for finishing cuts. The feedrate for finishing cuts was approximately 0.9 μm per revolution. Photographs of diamond turned aerogel appear in Figure 5. In the photographs, the aerogel is

illuminated by reflecting a light off a piece of blue paper located behind the aerogel. The chips generated in the cutting process can be seen sticking to the sides of the diamond cutting tool. Using this machining setup, several hemispheres of aerogel with an inner diameter of 216 μm and an outer diameter of 444 μm were fabricated.

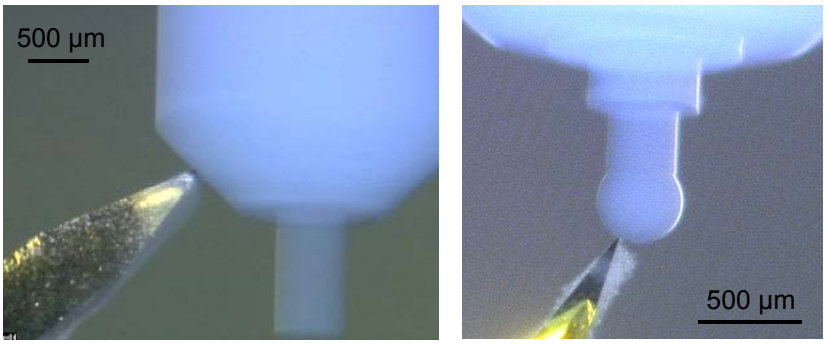

Figure 5. Diamond turning of SiO_2 aerogel

Several samples were created by assembling two of these aerogel hemispheres along with an inner capsule inside the ablator components. These samples were examined using an x-ray imaging system with a pixel pitch at the image of approximately 0.6 μm. The system uses a rotary table to rotate the sample and capture images at several angles. The data collected from this series of radiographs was then reconstructed to create a three-dimensional image of the sample [8]. Analysis of these tomographic reconstructions revealed that the aerogel had shifted and deformed in the assemblies, and an air-filled gap had formed between the two aerogel hemispheres. A radiograph showing a gap between the aerogel components in one of the assemblies appears in Figure 6.

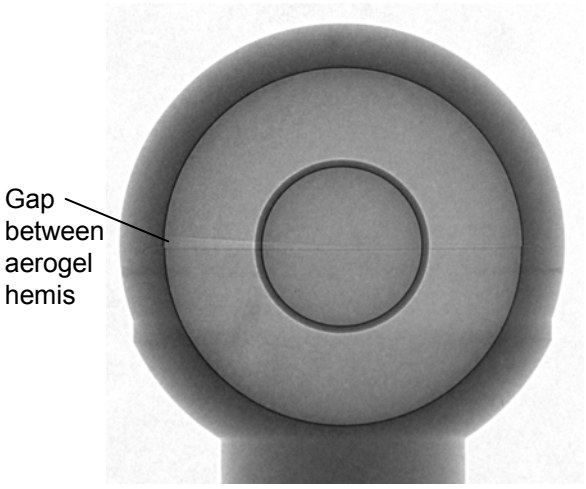

Figure 6. Radiograph of a gap between the aerogel components

During the assembly process, one or both of the aerogel pieces apparently had shifted as the upper ablator component was being put into place. This movement of the aerogel could have resulted from an electrostatic charge on either the plastic ablator components or the aerogel itself, or from the frictional interaction with the plastic. The low-density, compliant aerogel could then have deformed as the plastic ablator component was put into place, leaving a wedge-shaped gap between the two aerogel hemispheres. These gaps between the aerogel components were several μm wide and would have severely reduced the performance of the targets.

V.b. Current Method

To eliminate the possibility of any gaps forming between aerogel hemispheres, the manufacturing approach was altered so that the capsule was contained within a monolithic piece of aerogel. A process was developed in which the glass inner capsule was cast inside a block of SiO_2 aerogel. This process cast the aerogel into a 1 cm^3 cubic mold. The mold was first filled halfway with sol, which is a precursor to the aerogel. The sol was allowed to transform into a viscous gel, at which point the glass capsule was placed on the surface. The remainder of the cubic mold was then filled with sol, and the entire cube was allowed to transform into a gel. The mold was then placed into an autoclave, where the solvent was supercritically extracted, leaving the glass capsule embedded in SiO_2 aerogel of density 50 mg/cm^3. Some of these castings contained particles of higher density SiO_2 suspended in the aerogel, and some of them contained air-filled voids adjacent to the embedded capsule, which could be seen with an optical imaging system. Many of the castings used in the targets did not contain any particles or voids. However, because a limited number of glass capsules were available, some castings used in targets contained particles of up to 15 μm in diameter or voids of up to 8 μm adjacent to the capsule.

After casting the capsule inside a block of SiO_2 aerogel, the aerogel had to be machined into a sphere of diameter 444 μm that was concentric to the embedded capsule to within 2 μm. This machining operation was performed on a diamond turning machine, as shown in Figure 7. To machine the aerogel concentric to the capsule, the capsule had to be placed on the axis of rotation of the machine tool spindle. The radial runout of the capsule was determined using an optical system that viewed the capsule through the optically transparent aerogel while rotating the spindle at approximately 50 revolutions per minute. The optical system contained a 20× infinity corrected microscope objective lens and an NTSC video camera with 768 × 494 pixels. The camera was situated on a three-axis stage mounted on the diamond turning machine, such that the camera could be adjusted in three orthogonal directions with respect to the workpiece. Two capacitance probes measured the position of the camera as it was moved in the xz plane, which allowed the optical system to be used as a measuring microscope with approximately 1 μm precision.

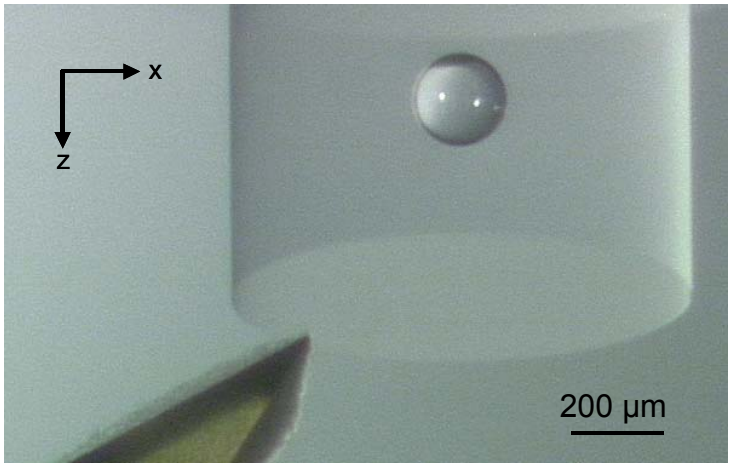

Figure 7. Diamond turning of SiO_2 aerogel cast around the inner capsule

Using this optical system, the position of the capsule was adjusted with respect to the spindle until there was no apparent radial runout. Determining the true runout of the capsule was complicated by the fact that aerogel refracts visible light, so the apparent position of the capsule

within the aerogel differed from the actual position. Next, several μm of aerogel were machined from the diameter of the part, and the apparent runout of the capsule was checked again. The process was repeated until a point was reached at which no noticeable capsule runout was observed after machining the outer diameter of the part.

With the capsule on the axis of rotation, a partial sphere of aerogel was then machined concentric to the embedded capsule, as shown in Figure 8. The measuring microscope mounted on the machine tool was used to ensure that the thickness of the aerogel at the pole of the sphere matched the thickness at the equator.

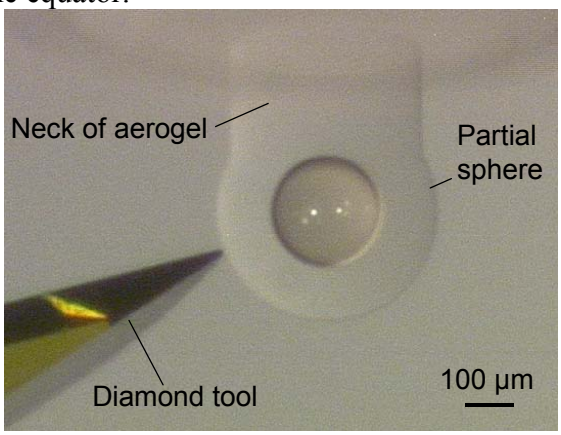

Figure 8. Diamond turning of the aerogel concentric to the embedded capsule

The sphere of aerogel was supported by a neck of material. After breaking the part off at the neck, the partial sphere of aerogel was then placed into a spherical vacuum chuck to machine off the neck, as shown in Figure 9. The spherical vacuum chuck was made of diamond turned brass, so both the part and the reflected image of the part are visible in the photograph.

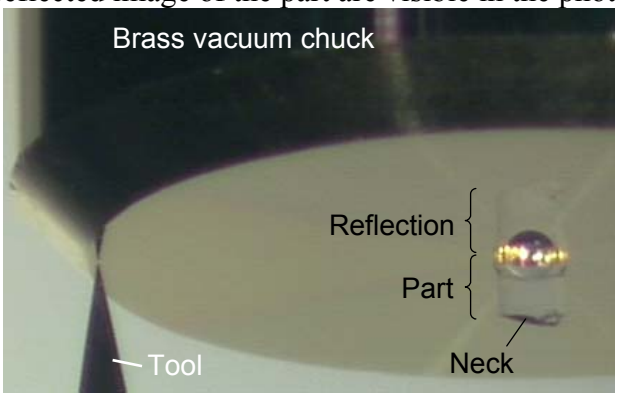

Figure 9. Partially finished aerogel component in a vacuum chuck

This process produced a sphere of aerogel containing the embedded capsule. A photograph of the aerogel after it has been machined to a sphere concentric to the embedded capsule appears in Figure 10. In this photograph, the sphere of aerogel is held by the diamond turned brass vacuum chuck, so both the part and the reflected image of the part are visible in the photograph. After completing the sphere, it remained in the vacuum chuck until it was assembled into the ablator components.

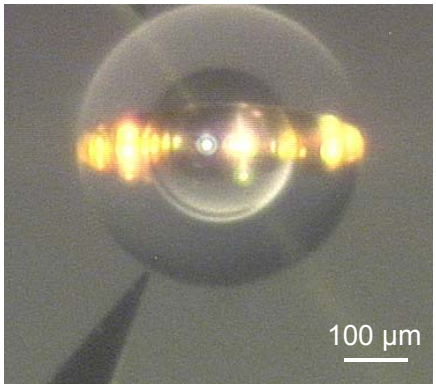

Figure 10. Aerogel sphere that has been machined concentric to the embedded capsule

VI. ABLATOR SHELL COMPONENTS

The ablator of the target consisted of two hemispherical shells of 2 atomic% bromine-doped polystyrene. The ablator shell had to be machined in two pieces in order to place the inner capsule and the aerogel inside of it. These hemispherical components mated at a step joint, which incorporated a gap that was partially filled with adhesive. Previous experience fabricating double shell targets revealed that if the ablator hemispherical shells are machined to their finished form as freestanding parts prior to assembling the targets, then it is difficult to bond them properly without getting adhesive on the exterior surface [9]. A cleaner and more precise exterior ablator surface can be obtained by assembling and bonding the target prior to machining the exterior surface of the ablator shell [2]. Therefore, the latter approach was used to fabricate these targets.

VI.a. Joint Design

The step joint between the two halves of the ablator shell is one of the most important design aspects of the targets. The manner in which the two ablator components fit together can have an important effect on the performance of the target. The joint represents a potentially significant asymmetry that could cause a non-uniform implosion and an unsuccessful experiment. Therefore, the joints had to fit together as precisely as possible.

The double shell targets fabricated and shot in 2003 used a step joint with a 2 μm gap that was partially filled with cyanoacrylate adhesive [2]. A schematic illustration of the joint used in the 2003 targets appears in Figure 11. The 2 μm gap was intended to be completely filled with cyanoacrylate. However, studies were performed in which ablator assemblies containing this joint design were bonded together using the same process used to bond the 2003 targets. The two ablator components were later pulled apart and revealed that the gap was only about half filled with adhesive.

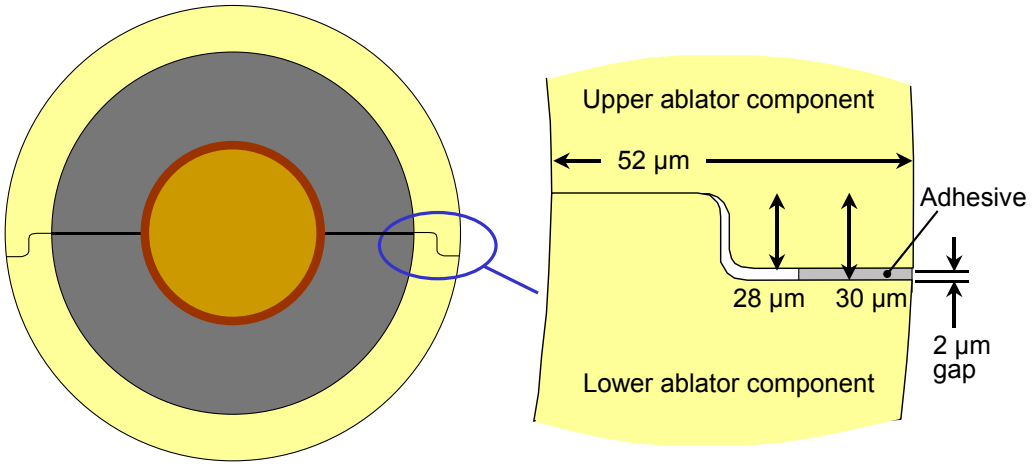

Figure 11. Joint design used in the 2003 double shell targets

Simulations have indicated that a 2 µm gap such as this could have noticeably reduced the performance of the target. Even if the gap had been completely filled with adhesive, it would have represented a significant asymmetry in the target. The 2 atomic% bromine-doped polystyrene has a density of 1.24 g/cm^3, which is significantly larger than the 1.0 g/cm^3 density of the cyanoacrylate adhesive. The bromine-doped polystyrene also has a significantly larger x-ray opacity than the adhesive. Therefore, a completely filled gap would constitute a 2 µm thick region of material with a density and x-ray opacity that differed from the base ablator material. A gap that was only filled about halfway with adhesive would have caused an even larger asymmetry in the target and reduced its performance even further. Therefore, the joint was redesigned for the current set of targets. Several studies were performed to identify a method of joining the two halves of the ablator shell with a seam that contributed the smallest possible asymmetry.

Several types of bonding agents were investigated as a replacement for cyanoacrylate. Solvent adhesives could theoretically be used to create a seamless joint between two pieces of plastic. A solvent adhesive could partially dissolve the ablator material so that the opposing ablator hemispheres would flow together as the solvent evaporated. This type of joint would not contain any materials with a density or x-ray opacity that differ from the ablator. Unfortunately, solvent adhesives could not be dispensed with adequate control over the volume applied to the target components. They tended to either not bond the components together, or to completely dissolve the material and ruin the carefully diamond turned interior of the ablator components. Bonds formed by epoxies did not have adequate strength. At the time this work was performed, other joining methods, such as friction welding, ultrasonic welding, or laser welding, were not practical for parts with this geometry.

Cyanoacrylate appeared to have the best bonding characteristics of all of the bonding methods considered. One method of reducing the asymmetry contributed by a cyanoacrylate bond is to minimize the size of the gap in the step joint, thereby minimizing the amount of material with a density and x-ray opacity that differ from the bromine-doped polystyrene. The smallest gap that could be reliably machined into the joint between the ablator components was 0.1 µm. The diamond turned ablator material had a peak-to-valley roughness on the order of 80 nm, and the gap should not be designed smaller than the roughness of the material. Therefore, the practical lower limit for the gap was set at 0.1 µm, and studies determined that a joint with a 0.1 µm gap could be adequately bonded using cyanoacrylate. A gap of this size was too small to

be modeled accurately in computer simulations to predict its exact effect on the performance of the targets. However, because this gap had only 5% of the volume of the gap used in the 2003 double shell targets, it represented a significant improvement to the joint design and was selected for the current set of targets. A schematic illustration of the joint design appears in Figure 12. The left side of Figure 12 is a cross sectional view that shows the inner capsule and aerogel sphere inside the unfinished ablator components, and it corresponds to Figure 2c.

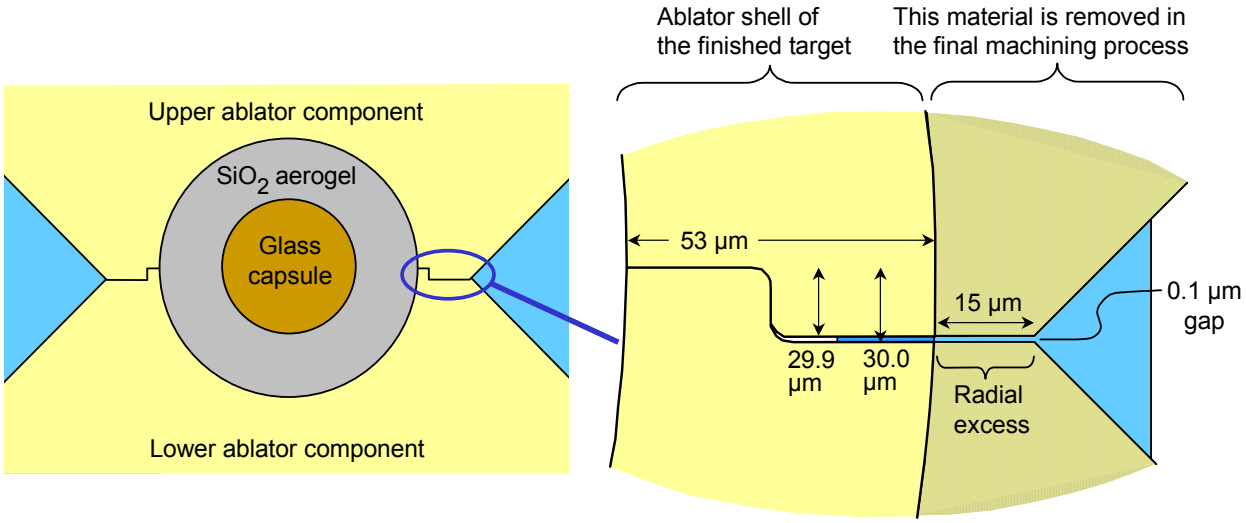

Figure 12. Assembled target components (left) and an enlarged view of the joint design (right)

The joint was carefully designed by considering the asymmetry that it creates in the targets, and by considering the ability to assemble, bond, and machine the ablator components. The step in the joint facilitated assembly by ensuring that the components were properly aligned radially. The chamfered sections facilitated the application of the adhesive. The dimensions and geometry of the step joint were designed around the curing properties of the adhesive. Each of these factors was crucial to successfully assembling and bonding the targets.

Recall that when fabricating these targets, they were assembled prior to machining the outer surface of the ablator components, as shown in Figure 2c and in the left side of Figure 12. After assembling all of the components, a small amount of adhesive was applied into the chamfered section near the joint. The chamfers in the ablator components provided surfaces for the adhesive to wick into the gap between the components. Every dimension of the step joint was selected to allow the adhesive to wick into the 0.1 μm gap between the components, so it would bond the ablator components together without wicking past the joint and into the aerogel in the spherical cavity. The shaded region on the right side of Figure 12 is a portion of the ablator material and cured adhesive that were machined off after the target was bonded. As shown in the figure, this "radial excess" was an extension of the 0.1 μm gap that spanned a length of 15 μm into the excess material.

The dimension of the radial excess played an important role in filling the joint with adhesive, because it determined the total distance that the adhesive traveled from the point of application to the point at which it cured. For a surface-activated adhesive, such as cyanoacrylate, the distance that the adhesive must flow and the ratio of surface area to volume play important roles in the wicking and curing of the adhesive. If the radial excess were too large, then the adhesive could have cured before reaching the inner 53 μm portion of the ablator

component that remained on the target. In this case, the bonded assembly would fall apart during the final machining operation. If the radial excess were too small, then the adhesive could have wicked past the step section of the joint and into the aerogel in the interior. In this case, the adhesive in the aerogel would have been an asymmetric feature that would have degraded the physics performance of the target. Trial and error revealed that a radial excess of 15 μm worked adequately for a 0.1 μm gap filled with LocTite 495 cyanoacrylate.

VI.b. Diamond Turning

In order for the target to perform correctly in the experiment, the inner surface of the ablator shell had to be smooth. Any misalignment or offset in the radial direction between the upper and lower ablator components had to be less than 0.5 μm. Therefore, each half of the step joint had to be machined with a precision of 0.25 μm. Figure 13 contains schematic illustrations of two possible configurations for the inner surface of the ablator at the interface between the ablator components. The left side of the figure illustrates a smooth ablator inner surface, which would result from properly machined ablator components. The right side of the figure illustrates a step discontinuity on the inner surface of the ablator, which would result from imperfect ablator components. A step discontinuity between the two halves of the ablator larger than 0.5 μm would create an unacceptable asymmetry that would significantly reduce the performance of the target.

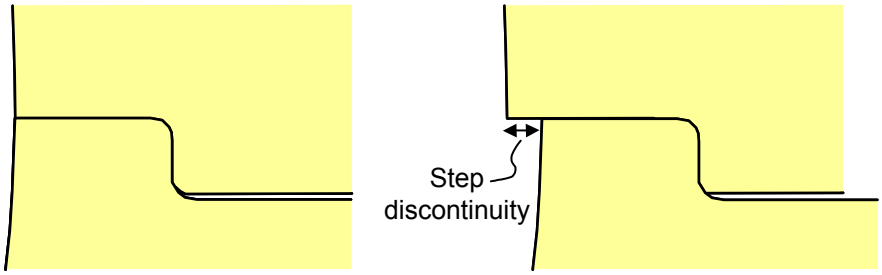

Figure 13. Enlarged views of the step joint illustrating a smooth inner surface of the ablator (left) and an ablator inner surface containing a step discontinuity (right)

Each component was machined on a Moore Nanotech 350 diamond turning machine using a diamond tool with a nose radius of 5 μm and a conical clearance with a primary clearance angle of 22°. The diamond turning machine has a rotary table (B-axis) that allows the cutting tool to swivel with respect to the workpiece. This rotary table is required to machine complicated features with a continuous tool pass, such as the hemispherical cavities and the step joint features.

In order to machine parts accurately, the cutting edge of the diamond tool had to be placed precisely on the axis of rotation of the rotary table. Any offset of the tool from the axis would create improperly sized parts and a step discontinuity on the inner surface of the ablator. To achieve the required precision of 0.25 μm on each of the ablator components, the cutting tool had to be positioned on the rotary table with an accuracy of approximately 0.1 μm. To facilitate positioning the tool with this level of accuracy, a special tool holder was developed that allowed the tool position to be precisely adjusted [10]. This tool holder incorporates flexure hinges and allows the tool position to be adjusted with 20 nm precision, so it could be set on the rotary table with the required accuracy in a reasonable amount of time.

Another significant obstacle to achieving the required machining accuracy was thermal drift of the diamond turning machine. The diamond turning machine was located in a facility whose ambient temperature was controlled to ±0.5 ºC. Several tests were performed to determine the drift experienced by the machine tool over the course of several days in this environment. The primary contributors to the thermal drift of the machine included variations in the air temperature, heat from the machine tool operators, heating and cooling associated with starting and stopping the spindle each time the workpiece was changed, and the heat generated by the linear motors that drive the machine tool slides. The tests revealed that the machine typically drifted more than 0.5 μm over the course of a day, and the trend was not consistent from one day to the next. However, if appropriate measures were taken to warm up the machine properly, then it usually did not drift more than about 0.1 μm in any one hour period.

To minimize the effects of machine tool drift on the relative size of mating ablator components, each pair of ablator component was machined in a specific sequence. Each ablator component was fabricated from a 6 mm diameter rod of 2 atomic% bromine-doped polystyrene. The end of each rod was first machined with a 45º chamfer. The interior surface was then machined in two steps. Initially, the hemispherical cavity and the step section of the joint were rough-machined into the material, leaving 10 μm of excess material on the part. When performing the final machining to remove this 10 μm of material to bring the part to the final size, each pair of mating components was machined as a set. The lower ablator component was inserted in the machine tool and was machined to its final size. It was then removed, and the upper ablator component was installed and machined to its final size. Because only a few tool passes were required to remove the last 10 μm of material, the two mating components could both be machined in less than an hour. Therefore, the machine tool was expected to experience thermal drift of up to approximately 0.1 μm during the finish machining of the components. A photograph of a completed lower ablator component appears in Figure 14.

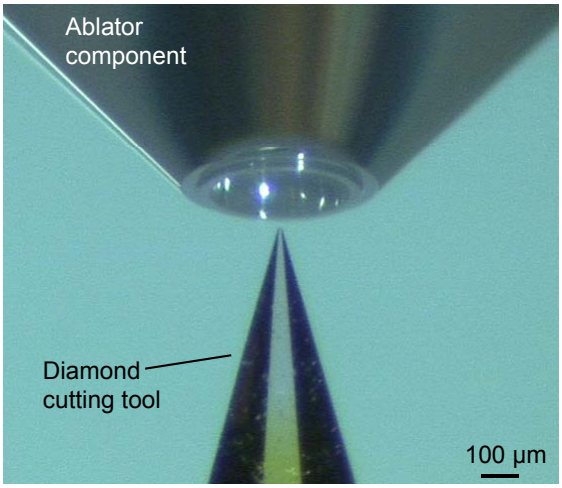

Figure 14. Diamond turned ablator component

VI.c. Characterization

In most manufacturing efforts, machined parts are measured to ensure that they are made to the proper size. To determine if the diamond turned ablator components would fit together properly, it would be necessary to measure the inner diameter of the hemispherical cavity of each part, the inner diameter of the sidewall of the step joint on the upper ablator component, and the

outer diameter of the sidewall of the step joint on the lower ablator component. Each of these measurements would have to be made with an uncertainty better than 0.1 μm. Due to the size of the parts, the complicated geometry of the features, and the viscoelastic nature of the workpiece material, there were no tools available that could make these measurements with adequate accuracy.

Although it was not possible to measure the ablator components prior to assembling a target, digital radiography systems were available that could nondestructively characterize a bonded assembly to determine the size of any step discontinuity on the inner surface of the ablator. One of the radiography systems, the XRT XuM system, uses a 20 kV x-ray point source, which produces a 9 keV characteristic x-ray. The system uses a 1340 × 1300 pixel scientific grade Charge Coupled Device (CCD) camera as a detector. The detector is used in a direct detection mode, and the pixel pitch of the CCD is 20 μm. For the geometric magnification required to examine the components, the effective pixel size of this digital radiography system was approximately 0.25 μm. Therefore, the system could determine if the inner surface of a set of ablator components contained a step discontinuity greater than 0.5 μm. This system could be used to inspect a set of ablator components after they had been bonded together. However, if the system revealed that the components had not been machined within the specifications, it was too late to make any adjustments to these parts.

To establish confidence in the machined dimensions of a set of ablator components prior to assembling it with an expensive aerogel-capsule subassembly, quality control measures were used. As the ablator components were being diamond turned, several extra sets were machined at the same time. Each extra set was used to make a dummy assembly that was bonded without placing anything in the interior. The dummy assembly was then examined with the radiography system. If the dummy assembly was acceptable, then the accompanying sets of ablator components were used to make targets. If the dummy assembly contained an unacceptable step discontinuity on the inner surface, then the accompanying ablator sets were discarded. Based on the magnitude and nature of the error observed in the dummy assembly, it was often possible to determine the cause of the problem and correct it. Using this method, seven sets of ablator components were machined and used to make double shell targets.

VII. ASSEMBLY AND BONDING

The components were assembled using a special assembly station that incorporates a force sensor to allow the operator to control the assembly forces to within a few milliNewtons. The assembly station consists of two sets of actuators that allow the mating components to be aligned and then assembled. One of the mating components to be assembled is installed on the lower set of actuators, which consists of a set of stages that are driven by manual micrometers with a resolution of 1 μm. This set of stages allows the part to be oriented radially, and two perpendicular microscopes allow the operator to visually determine when the parts are aligned.

The other component is installed on the upper set of actuators. This set of actuators provides fine motion in the axial direction to assemble the components. This set of actuators was designed to provide control over the assembly forces to within a few milliNewtons by providing controlled compliance in the axial direction, which is created by a spring and a force transducer coupled to an air bearing.

The assembly process for the target, which is schematically illustrated in Figure 2 and Figure 3, is depicted in Figure 15. First, the lower ablator component was placed into the assembly station. The aerogel sphere containing the embedded glass capsule was then placed

into the hemispherical cavity in the lower ablator component (Figure 15a). The upper ablator component was then placed over the aerogel to complete the assembly (Figure 15b). The components were then pressed together with a force of 0.2 N. A droplet of cyanoacrylate was picked up on the end of a hair and applied to the seam between the components. The adhesive quickly wicked around the chamfered section of the components to seal the target, as shown in Figure 15c. The cyanoacrylate was intended to fill the 0.1 μm gap between the ablator components without flowing past the step joint section of the ablator components and into the aerogel.

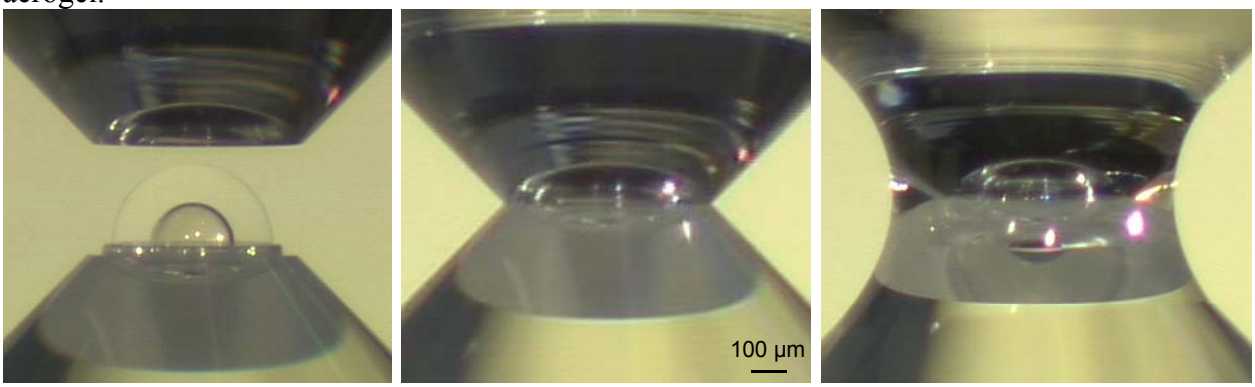

Figure 15. Assembly and bonding of a target

After allowing the cyanoacrylate to cure for an hour, the tapered sections of the components were filled with epoxy, which was allowed to cure for 24 hours. This epoxy supported the joint during machining and was fully machined away in subsequent steps.

VIII. MACHINING THE FIRST HALF OF THE ABLATOR EXTERIOR

After the target components were assembled and bonded, the exterior of the ablator shell was diamond turned, as illustrated in Figure 3. Initially, only the first half of the exterior of the ablator was machined to create a partial sphere with a uniform wall thickness. For the target to implode correctly, the thickness of the ablator shell had to be uniform to ±1 μm. In order to machine the outer surface of the ablator concentric to the inner surface, the assembly had to be placed back on the axis of rotation of the machine tool spindle. A reference diameter that had been machined on the brass stub that supported the bromine-doped polystyrene facilitated this process. Once the part was aligned on the spindle, material was removed to begin machining the 2.5 mm diameter ablator components to a 550 μm diameter target. A reference surface, which was used in a subsequent machining operation, was machined near the base of the partial sphere.

Achieving the required wall thickness uniformity was complicated by the fact that the plastic material deformed as it was machined. Although the plastic stock material had been heat treated prior to performing any machining, most plastics contain residual stresses. When machining the part, these residual stresses can be relieved, causing the part to deform. The part may shift with respect to the axis of rotation by as much as several μm during machining.

In order to obtain an ablator shell with uniform wall thickness, it was radiographed prior to the final tool passes. The part was initially machined to a partial sphere with a diameter greater than 600 μm. The brass stub that supported the plastic was then diamond turned to create a reference surface concentric to the machined exterior of the part. The part was then removed from the machine tool and placed in the digital radiography system. Several digital radiographs

were taken of the part to determine the magnitude and direction of any eccentricity between the inner and outer surfaces of the ablator shell. Figure 16 contains digital radiographs that were taken with two different x-ray systems at this point in the process. The digital radiograph on the left was acquired with an x-ray point projection system developed by Xradia, Inc. called MicroXCT. The digital radiograph on the right was acquired with the XuM system.

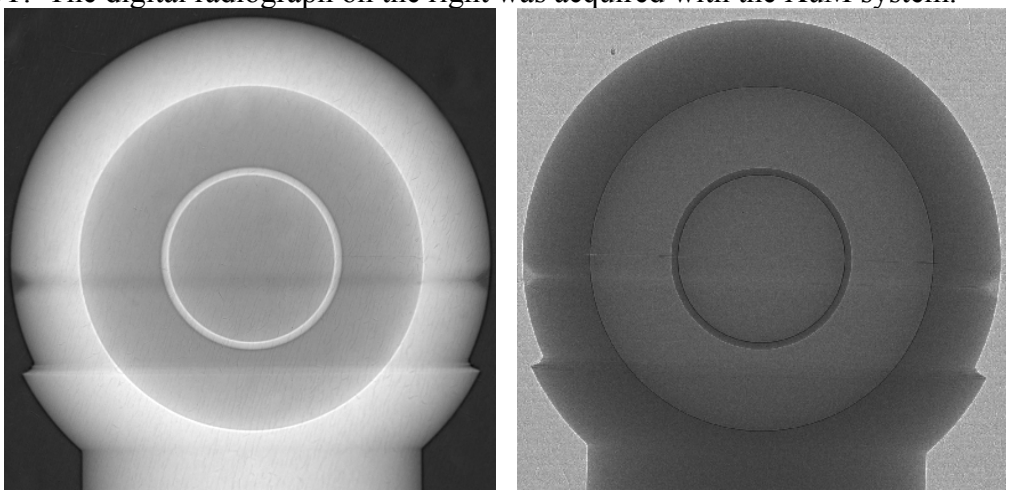

Figure 16. Attenuation digital radiograph taken with the MicroXCT system (left) and transmission digital radiograph taken with the XuM system (right) of an unfinished double shell target

The part was then placed back on the diamond turning machine. A capacitance probe was placed adjacent to the reference diameter on the brass stub, and the radial location of the part was adjusted until the radial runout of the brass matched the observed eccentricity of the ablator shell. The part was then machined to a partial sphere of diameter 550 μm, as shown in Figure 17.

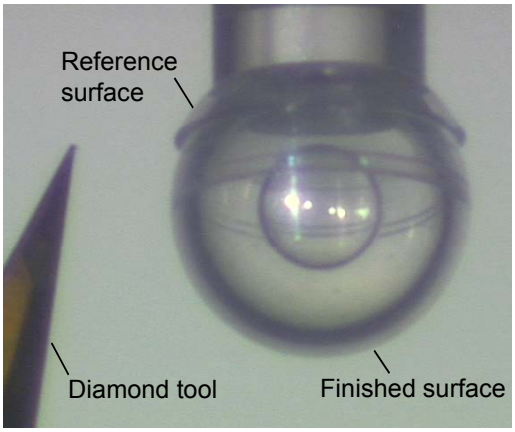

Figure 17. Partial sphere machined on the ablator exterior

IX. CHARACTERIZATION

At this point in the manufacturing process, two-thirds of the outer surface of the target had been machined to its final form, and the target was mounted on a stalk. This configuration was convenient for characterizing the partially finished target using several digital radiography systems.

Each target was first examined with the MicroXCT tomography system. This system uses a 150 kV x-ray source operating at 100 kV. Along with the Bremsstrahlung spectra, the

tungsten anode produces two characteristics, one at approximately 9 keV and the other at approximately 59 keV. The 9 keV x-ray is the predominant characteristic. The detector consists of a CsI scintillator mounted on a 20× microscope objective, which is optically coupled to a scientific grade 2048 × 2048 CCD array. With geometric magnification, the system has an effective pixel size of 0.57 μm. The actuator holding the target consists of a three-axis linear stage mounted on a rotation stage. Using this system, a total of 721 images were taken of each target at 0.25º intervals. Computed Tomography (CT) software developed at LLNL was then used to create volumetric reconstructions of the data [8]. Images of the tomographic slices made of the reconstructed data appear in Figure 18. The image on the left side of the figure is a slice through the data from the pole to the stem. The image on the right side of the figure is a slice made through the data near the seam between the ablator components. Wall thickness uniformities of the finished ablator shell were made from three orthogonal CT slices. For the seven targets that were manufactured, the wall thickness uniformities ranged from ±0.25 to ±0.9 μm. The data was also used to volumetrically calculate the concentricity between the outer surface of the inner shell and the inner surface of the ablator shell. The concentricity between the two shells was required to be less than 3 μm, and the measured values on the seven targets all met this requirement and ranged from 0.1 to 1.4 μm.

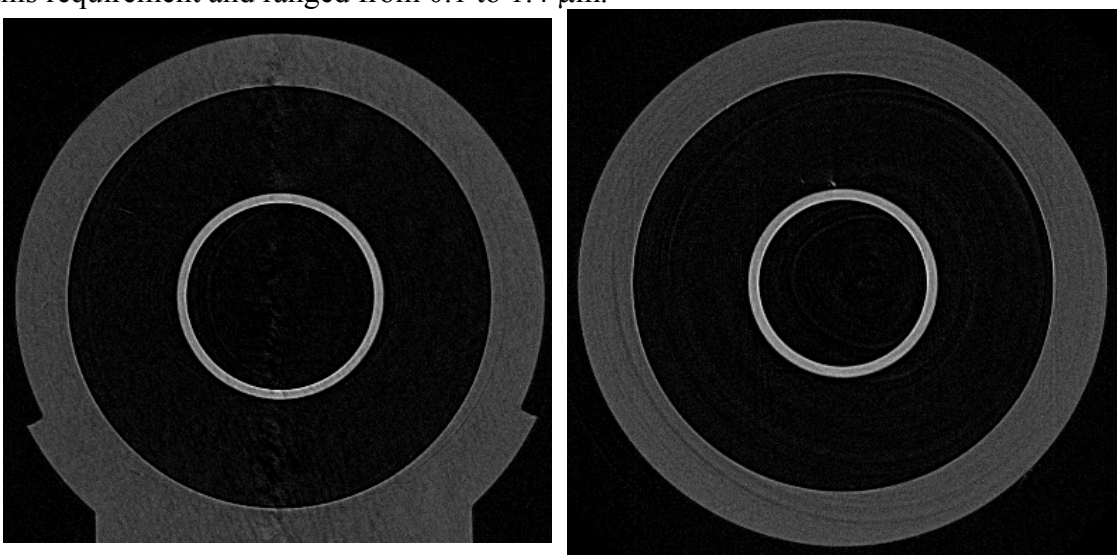

Figure 18. Computed tomography slices of a double shell target

Each target was also examined with the XuM system to measure the size of the step discontinuity on the inner surface of the ablator shell and to identify any gaps in the joint. Digital radiographs taken with the XuM system appear in Figure 19. The image on the left was taken before the target was complete and verifies that the inner surface of the ablator was smooth and did not contain an unacceptable step discontinuity at the interface between the ablator components. The feature to the right of the capsule in this digital radiograph is a piece of debris that was stuck to the electron shield that was placed over the parts to protect them from stray electrons created in the system. This digital radiograph corresponds to the maximum possible magnification of the system, which was limited by an inability to move the sample any closer to the x-ray source. Images such as this one were taken every 45º around the joint. The image on the right side of Figure 19 is a lower magnification digital radiograph of the entire part and was taken after the first half of the ablator had been machined to its final thickness of 53 μm.

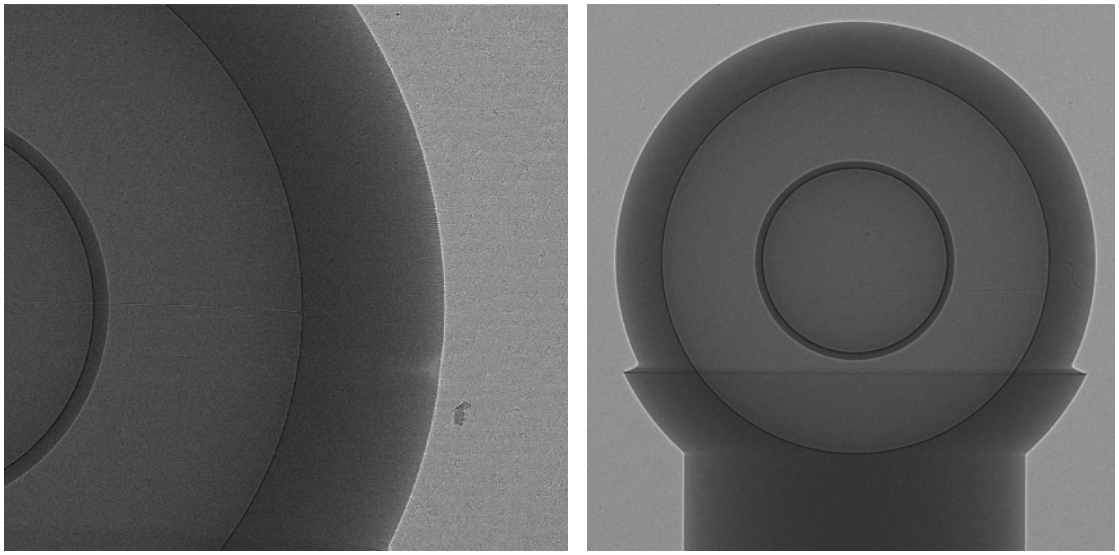

Figure 19. Digital radiographs taken with the XuM system

The targets were also examined with the Xradia, Inc. nanoXCT x-ray zone-plate based imaging system. This system has a field of view of 17 μm and a pixel pitch of 17 nm. The images were taken with a 2 × 2 detector bin to increase the signal-to-noise ratio and shorten the exposure time. The detector binning resulted in a pixel pitch of 34 nm. Using the nanoXCT system, the interface between the two ablator components of each target was inspected at 90º intervals around the joint. Images taken with the XuM and nanoXCT systems revealed that six of the seven targets that were manufactured met the requirement for a smooth inner ablator surface. For these targets, the step discontinuities at the inner surfaces of the ablators were less than the specification of 0.5 μm, and they ranged from 0 to 476 nm. The uncertainty in these measurements was limited by the size of the pixels in the images, which was 34 nm for the nanoXCT system. The seventh target contained a step discontinuity of approximately 100 nm around the majority of the seam, with a step discontinuity of 690 nm at a single location, which may have been caused by debris on one of the components prior to assembly.

The images taken with the nanoXCT and the XuM systems were also used to determine how well the ablator components were seated against each other at the joint. On four of the seven targets, the two components appeared to mate flush with each other all the way around the joint. On the other three targets, the ablator components mated flush with each other around the majority of the perimeter, but there was a gap extending approximately 45º around the perimeter of the seam where the inner sections of the step joint were not in contact. This separation between the ablator components ranged in thickness from 0.5 μm to approximately 1 μm and was probably caused by debris, such as chips or dust, on one of the ablator components prior to assembly.

X. MACHINING THE FINAL HALF OF THE ABLATOR EXTERIOR

The final machining operation performed on the target was to remove the stem and diamond turn this side of the target to a spherical contour. The target was placed back on the diamond turning machine, where the neck holding the partial sphere was machined to a diameter of approximately 100 μm, as illustrated in Figure 3e. This thin neck was then severed with a surgical blade, and the target was placed in a hemispherical vacuum chuck, as illustrated in Figure 3f. Because the part was so small, vacuum alone did not provide sufficient holding torque

to prevent the part from slipping as a result of the forces imposed by the cutting tool. Therefore, to augment the grip of the vacuum chuck, droplets of urethane adhesive were applied to bond the part to the chuck, as illustrated in Figure 3f. The second half of the outer contour of the target was then machined to shape the ablator into a complete sphere with a wall thickness of 53 μm. A photograph of the target being held in the vacuum chuck and secured with urethane appears in Figure 20.

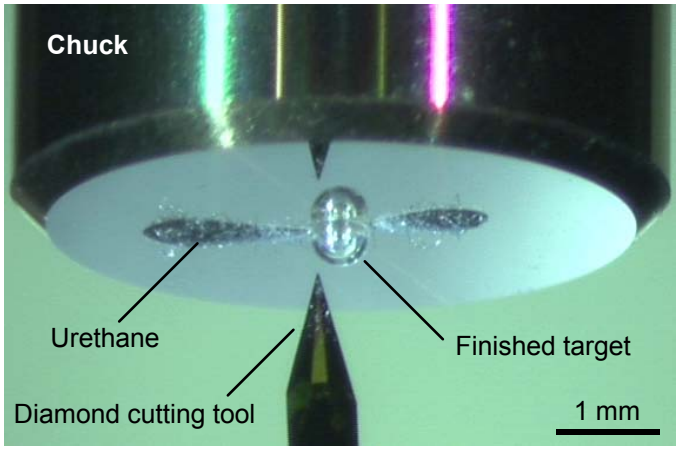

Figure 20. Diamond turning of the final half of the ablator exterior

After all machining was complete, the urethane was peeled off so that the completed target could be removed from the chuck. Small pieces of urethane sometimes stuck to the exterior of the target and had to be carefully removed with a foam swab. A photograph of a finished target appears in Figure 21. The final operation was to tent the target in Formvar and mount it in a hohlraum. The complete assembly was then pressurized to diffusion fill the inner glass capsule with 62 atm of deuterium.

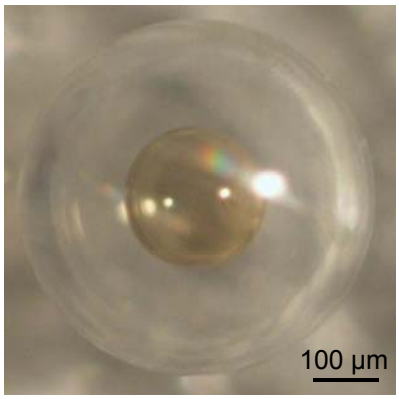

Figure 21. Finished double shell target

XI. DISCUSSION

The manufacturing process developed for these double shell targets represented a significant improvement to previous work. A number of technological advances were made that allowed these targets to be manufactured with the required accuracy. This work also identified many potential improvements and additional advances that could be made to fabricate even better targets.

A method was developed for casting the glass inner capsules in a block of SiO_2 aerogel of density 50 mg/cm^3. This development eliminated a significant problem that occurred in previous work when a void formed between freestanding aerogel hemispheres that were assembled around the glass capsule. The monolithic piece of aerogel containing the capsule also simplified the assembly process by reducing the number of components that had to be aligned. Although this new casting process was a significant achievement that was critical to the success of this manufacturing effort, it could be improved to produce even better double shell targets. Some of the castings contained particles of higher density SiO_2 at the interface between the two pours. These particles ranged in size from a few μm to more than 15 μm in diameter. These particles probably formed when the mold was half filled and the capsule was inserted. Portions of the sol-gel probably began to condense while exposed to air at the surface. After filling the mold with the second pour and extracting the solvent, these particles formed xerogel with a density greater than that of the aerogel. Other castings contained an air-filled void adjacent to the capsule, which probably formed as the capsule moved with respect to the gel as the second half of the mold was filled. These issues could be solved by developing a new sequence for the casting of the aerogel around the glass capsule.

Methods were developed to diamond turn SiO_2 aerogel of density 50 mg/cm^3 to a spherical form concentric to the embedded glass capsule. This achievement required identifying a formulation that produced an aerogel material robust enough to be machined. It also required the development of a method to machine the aerogel concentric to the embedded capsule. A measuring microscope was constructed and mounted on the machine tool to allow parts to be measured with an uncertainty of approximately ±1 um. This hardware was used to machine the aerogel concentric to the embedded glass capsule and produced targets in which the two shells were concentric to l.4 μm or better.

The ablator components on these double shell targets were significantly more precise than those of previous targets. A new step joint was designed for the interface between the two ablator components. This step joint included a gap with a nominal thickness of only 0.1 μm that was partially filled with cyanoacrylate. This new gap had a volume of only 5% of the 2 μm gap used on the targets shot in 2003. The inner surface of each ablator shell was adequately smooth. Step discontinuities in excess of 1 μm that had been observed in previous efforts were reduced, as required, to less than 0.5 μm. This new level of precision was due in part to a special tool holder that was developed to facilitate positioning the diamond cutting tool precisely on the axis of the rotary table (B-axis) of the diamond turning machine.

These double shell targets were nondestructively characterized using a number of x-ray methods. X-ray data were acquired using the MicroXCT, nanoXCT, and XuM systems. The x-ray data were used to characterize the concentricity of the inner shell to the ablator shell, the size of any step discontinuity on the inner surface of the ablator, and the wall thickness uniformity of the ablator shell. This new level of nondestructive characterization allowed several flaws in the targets to be identified, so the manufacturing process could be adjusted to eliminate the flaws. In addition, the raw x-ray data and the reconstructed datasets were used not only to certify that the finished targets met all of the requirements, but they were also used to provide feedback at various stages of the manufacturing process. Although the feedback from the x-ray data allowed the targets to be manufactured to the specifications, the process was expensive and inefficient. The manufacturing process would have been more efficient if quantitative metrology tools had been available. For example, to ensure there was no step discontinuity on the inner surface of the ablator, the step joints each had to be machined with a precision of 0.25 μm. However, no

metrology tools were available that could adequately make these measurements on the step joints before the components were assembled. Advanced meso-scale metrology tools would benefit not only double shell targets, but the manufacture of all meso-scale laser targets with complex geometries.

XII. SUMMARY

Lawrence Livermore National Laboratory has made several technological advances that have led to double shell targets that represent a significant improvement to previously fielded targets. The inner capsule was supported inside the ablator shell by SiO_2 aerogel with a nominal density of 50 mg/cm^3. Methods have been developed to machine, handle, and assemble this fragile material. The inner capsule was cast into a block of aerogel, which was then machined into a spherical form around the embedded capsule. Measuring microscopes mounted on the machine tool enabled the aerogel to be machined to a sphere concentric to the embedded capsule to within approximately 1 μm. The ablator consisted of two hemispherical shells that mated at a step joint that incorporated an adhesive-filled gap with a nominal thickness of 0.1 μm. A new flexure-based tool holder for precisely positioning the diamond cutting tool on the rotary table of the diamond turning machine led to step discontinuities on the inner surface of the ablator of less than 0.5 μm. The concentricity between the two shells was improved to 1.4 μm or better. New methods were used to comprehensively characterize each of the targets using high-resolution x-ray imaging systems.

ACKNOWLEDGEMENTS

This work would not have been possible without the skill of the machinists, Don Bennett and Carlos Castro. Joe Satcher, Stuart Gammon, Bob Reibold, and John Poco provided the materials for these targets. John Poco cast the glass inner capsules in aerogel. Bill Brown and Nick Teslich performed x-ray characterization. Bill Brown and John Sain reconstructed and processed the tomographic data. Dave Swift helped analyze digital radiography data. Software used to reconstruct and analyze x-ray data was developed by LLNL's Center for Nondestructive Characterization, which is directed by Harry Martz, and by LLNL's Radiation Applications Group, which is lead by Diane Chinn. Russell Wallace also contributed to the production of these targets. And finally, Lee Griffith, Jeff Kass, Alex Hamza, and the other members of LLNL's Target Fabrication Team contributed to this work.

This work was performed under the auspices of the U.S. Department of Energy by UC, Lawrence Livermore National Laboratory under contract W-7405-ENG-48.

REFERENCES

[1] P. A. Amendt, H. F. Robey, H.-S. Park, R. E. Tipton, R. E. Turner, J. L. Milovich, M. J. Bono, R. L. Hibbard, H. Louis, R. Wallace, "Hohlraum-Driven Ignitionlike Double-Shell Implosions on the Omega Laser Facility," *Physical Review Letters* **94**, 065004 (2005).

[2] R. L. Hibbard, M. J. Bono, P. A. Amendt, D. W. Bennett, and C. Castro, "Precision Manufacturing of Inertial Confinement Fusion Double Shell Laser Targets for OMEGA," *Fusion Science and Technology* **45**, 2, 117-123 (2004).

[3] C. W. Hatcher, L. E. Lorensen, B. W. Weinstein, "Double-Shell Inertial Confinement Fusion Target Fabrication," *Journal of Vacuum Science & Technology* **18**, 3, 1187-1190 (1981).

[4] T. Norimatsu, A. Furusawa, M. Yoshida, Y. Izawa, C. Yamanaka, "Fabrication of Double Shell Targets for Laser Fusion," *Journal of Vacuum Science & Technology* **18**, 3, 1288-1289 (1981).
[5] K. R. Schultz, J. L. Kaae, W. J. Miller, D. A. Steinman, R. B. Stephens, "Status of Inertial Fusion Target Fabrication in the USA," *Fusion Engineering and Design* **44**, 441-448 (1999).
[6] J. R. Duke, N. E. Elliott, J. E. Moore, V. M. Gomez, R. Manzanares, G. Rivera, R. Watt, W. S. Varnum, P. L. Gobby, "The Fabrication of Double Shell Targets for Nova," *Fusion Technology* **35**, 2, 90-94 (1999).
[7] R. L. McEachern, C. E. Moore, R. J. Wallace. "The Design, Performance, and Application of an Atomic-Force Microscope-Based Profilometer," *Journal of Vacuum Science & Technology A-Vacuum Surfaces and Films* **13**, 3, 983-989 (1995).
[8] W. D. Brown, H. E. Martz, "X-ray Digital Radiography and Computed Tomography of ICF and HEDP Materials, Subassemblies and Targets," *Digital Imaging IX, An ASNT Topical Conference*, Mashantucket, CT, July 24-26, 2006.
[9] M. J. Bono, R. L. Hibbard. "Machining, Assembly, and Characterization of a Mesoscale Double Shell Target," *Journal of Manufacturing Processes* **6**, 97-106 (2004).
[10] M. Bono, R. Hibbard. "A Flexure-based Tool Holder for Sub-μm Positioning of a Single Point Cutting Tool on a Four-axis Lathe," accepted for publication in *Precision Engineering: Journal of the International Societies for Precision Engineering and Nanotechnology*.